Am J Cancer Res 2020;10(2):491-506
www.ajcr.us /ISSN:2156-6976/ajcr0106043

Original Article

Histone demethylase KDM4C activates HIF1α/VEGFA signaling through the costimulatory factor STAT3 in NSCLC

Xiaowei Wu[1], Yu Deng[1], Yukun Zu[1], Jin Yin[2]

Departments of [1]Thoracic Surgery, [2]Hematopathology, Tongji Hospital, Tongji Medical Collage of Huazhong University of Science and Technology, Wuhan, Hubei Province, China

Received December 7, 2019; Accepted December 29, 2019; Epub February 1, 2020; Published February 15, 2020

Abstract: Tumor development is accompanied by high hypoxia and a dense network of immature vessels. The hypoxia-inducible factor/vascular endothelial growth factor (HIF/VEGF) signaling pathway is activated in various solid tumors. It is thought that HIF/VEGF signaling activation results from intratumoral hypoxia partly. Multiple studies have reported that VEGF is a common target gene for both transcription factors STAT3 and HIF1. KDM4C has also been reported to function as a co-activation factor for HIF-1β/VEGF signaling activation. In this manuscript. Our results demonstrate that KDM4C promotes NSCLC tumor angiogenesis by transcriptionally activating HIF1α/VEGFA signaling pathway. We also find that STAT3 functions as a costimulatory factor in this process. This pathway opens a potential therapeutic window for the treatment of NSCLC.

Keywords: Tumor angiogenesis, NSCLC, KDM4C, HIF1α, STAT3

Introduction

Globally, lung cancer is the most common malignancy and the leading cause of cancer deaths (Cancer Today-IARC, 2018). In 2018, lung cancer caused close to 1.8 million deaths worldwide (Cancer Today-IARC, 2018). About 80-85% lung cancers are classified as non-small cell lung cancer (NSCLC) [1, 2]. Targeted Therapies are available for the treatment of advanced lung cancer, including Afatinib, a kind of small molecule inhibitor of EGFR [3]. Although antiangiogenic therapy is currently available in the clinic for the treatment of late stage lung cancer patients, resistance to such treatments frequently emerges [4-6]. Further limiting the treatment options available to the patient. Therefore, further investigation into the mechanisms of tumor angiogenesis is warranted in order to elucidate novel and more effective therapeutic strategies against NSCLC.

The hypoxia-inducible factor/vascular endothelial growth factor (HIF/VEGF) signaling pathway has been reported to be activated in various solid tumors. It is thought that HIF/VEGF signaling activation results from intratumoral hypoxia and/or an abnormal functioning of genes that promotes tumor angiogenesis [7, 8]. Apart from the abnormal activation of the HIF/VEGF signaling pathway, aberrant activation of the STAT3 (signal transducer and activator of transcription 3) has also been observed in various solid tumors, including those affecting the kidney, lung, breast and the head & neck tumor region [9]. In addition, multiple studies have reported that VEGF is a common target gene for both STAT3 and HIF1, and both transcription factors modulate VEGF expression during hypoxia [10-12]. Together, these observations imply an association between STAT3 and HIF1 in the regulation of tumor angiogenesis.

KDM4C, also known as JMJD2C (histone demethylase JMJD containing protein 2C) is encoded by the KDM4C gene and has been shown to be a transcription target of HIF1 [13]. KDM4C has been shown to demethylate lysine 9 of histone H3 (H3K9me2 and H3K9me3) and lysine 36 of histone H3, (H3K36me2 and H3K36me3) in vitro and in cells overexpressing KDM4C [14-16]. It has been reported that

KDM4C drives the proliferation and transformation of various cancer cells, including breast and leukemia cells [14, 17-19]. KDM4C has also been reported to function as a co-activation factor for HIF-1/VEGF signaling activation in breast cancer cells [20]. However, the function of KDM4C in NSCLC has not been previously interrogated.

In this study, we investigated the role of KDM4C in NSCLC using eighty NSCLC and eighty matched normal control clinical tissues. Our analyses revealed that KDM4C was significantly upregulated in NSCLC tumors relative to the matching normal, paracancerous tissues. We demonstrated that KDM4C demethylated both H3K9me3 and H3K36me3 in the HIF1α gene promoter region and activated the expression of HIF1α. Moreover, we found that KDM4C overexpression promoted proliferation, migration, and invasion of NSCLC cells in vitro as well and their growth in vivo, in a mouse xenograft model. Furthermore, we demonstrated that KDM4C cooperated with STAT3 as its costimulatory factor, in the modulation of HIF1α expression by KDM4C. Knocking down STAT3 or inhibiting its activation, suppressed the demethylation of H3K9me3 and H3K36me3 on the HIF1α gene by KDM4C in NSCLC cells. These findings enhanced our understanding of the molecular mechanisms of tumor angiogenesis. Our report suggested that the KDM4C/STAT3/HIF1α/VEGFA signaling pathway presented a novel therapeutic window for targeting tumor angiogenesis in the treatment and/or management of NSCLC.

Materials and methods

Cell lines and culture

The cell lines HEK 293 T, H460, HCC827 were obtained in the American Type Culture Collection (ATCC, Manassas, VA, USA). All cells were cultured at 5% CO_2 and 37°C with Dulbecco's modified Eagle's medium (DMEM) supplemented with 10% fetal bovine serum (Thermo Fisher Scientifific, Shanghai, China). For hypoxic conditions, cells were cultured in the hypoxic chamber (Coy Laboratory Products, Inc.) in the presence of 1% O_2, 5% CO_2, and 94% N_2 at 37°C. Y705 STAT3 phosphorylation was abrogated by adding 200 μM S3I-201 (sc-204304; Santa Cruz, Dallas, TX, USA) to media for 2 hours before hypoxia treatment.

Clinical samples

Primary tumor samples and the matched adjacent normal tissue were collected form NSCLC patients and restored in -80°C until used. Eighty NSCLC tumor and eighty matched normal controls were analyzed. Tissues from this study were obtained from Tongji hospital, Tongji medical college of Huazhong University of Science and Technology. This study was approved by the Huazhong University of Science and Technology Ethics Committee.

Antibodies and reagents

Antibodies for HIF1α (sc-71247), HIF1β (sc-55526), STAT3 (sc-8019), STAT3 Y705 phosphorylation (sc-8059), GAPDH (sc-47724), Histone3 (sc-517, 576), mouse IgG (sc-69, 786), and KDM4C (sc-515767) were obtained form Santa Cruz Biotechnology (Santa Cruz, CA, USA). VEGF-A (ab52917) were purchased from Abcam (Cambridge, MA, USA). The human VEGF-A ELISA Kit (EK0541) was purchased from BOSTER Biological Technology (Wuhan, China). H3K36me3 (#4909) and H3K9me3 (#13969) antibodies were purchased from Cell Signaling Technology (Danvers, MA, USA).

Western blot and immunoprecipitation (IP)

Cells were then lysed with NP40 lysis buffer supplemented with protease inhibitors and phosphatase inhibitors. Protein concentration was determined using the BCA protein assay kit (Thermo) following the manufacturer's instructions. Protein samples were then separated by SDS-PAGE. Next, proteins were transferred onto PVDF membranes. The membranes were then blocked by incubating in 5% milk in TBST for 1 hour, at room temperature. The membrane was then incubated with indicated primary antibodies overnight at 4°C. Following primary antibody incubation, the membranes were washed three times, 15 minutes per wash, with TBST buffer to remove excess antibody. The membranes were next incubated with HRP-conjugated secondary antibodies at room temperature for 1 hour. Following secondary antibody incubation, signal was developed using chemiluminescence substrate following the manufacturer's instructions.

Immunoprecipitation

For immunoprecipitation, clear cell lysates were prepared by NP40. The clear lysates were

then incubated with the indicated antibodies or control IgGs overnight at 4°C. The antibody incubated lysates were then incubated with protein A/G beads for 2 hours at 4°C while rotating. The beads were then washed three times using NP-40 lysis buffer and analyzed by western blot analysis.

Cell viability assay

Cell viability assays were done using the CCK8 cell viability kit. Briefly, NSCLC cells were seeded in 96-well plates (5×10^3 cells/well) and 10 μl of CCK8 added into each well, followed by incubation a humidified incubator for 3 hours at 37°C, 5% CO_2. Following the incubation, absorbance was measured at 450 nm using a Thermomax microplate reader.

Flow cytometry

For flow cytometry, Cells were seeded in 6-well plates and cultured to 90% confluence. For flow cytometry, the cells were fixed in iced 80% ethanol overnight at -20°C. Next, cells were washed three times using 1×PBS. DNA was stained by incubating the fixed cells with 5 mg/ml of propidium iodide diluted in 1×PBS containing RNase, at room temperature for 1 hour, away from light. Cell cycle analysis was then using a Becton-Dickinson FACScan System (Franklin Lakes, NJ, USA).

Real-time PCR assay (RT-PCR)

Total RNA was extracted using TRIzol Reagent and reverse transcription was performed using an RT-PCR kit according to the manufacturer's instructions. Quantitative PCR was performed using an ABI 7300 real-time PCR system (Applied Biosystems). The following primers (5'-3') were used: KDM4C: forward cgaggtggaaagtcctctgaa, reverse gggctcctttagactccatgtat. GAPDH: forward ggagcgagatccctccaaaat, reverse ggctgttgtcatacttctcatgg. The fold-change in gene expression was calculated using the 2^-ΔΔCT method using GAPDH as the housekeeping reference gene.

Immunohistochemistry (IHC)

Humans NSCLC samples were obtain form Tongji Hospital. The procedures followed standard manufacturer's protocols as described previously. Two experienced pathologists evaluated and reviewed immunostaining results independently. IRS system was used to quantify IHC staining by multiplying a proportion score and an intensity score. The proportion score reflected the fraction of positively stained tumor cells: 1 (<10%); 2 (10%-50%; 3 (50-75%); 4 (>75%). the intensity score revealed the staining intensity (0, no staining; 1, weak; 2, intermediate; 3, strong). Finally, the staining score ranged from 0 to 12.

ChIP assay

Cells were exposed to 1% O_2 for 24 h, cross-linked with 1% formaldehyde for 20 min at 37°C, and stop the reaction with 0.125 M glycine. DNA was immunoprecipitated from the sonicated cell lysates. The HIF1α primers used for CHIP assays were as follows: forward primer: 5'-AAGTTCTTGATATAACTGAAA-3', reverse primer: 5'-ATTGCTTGAAGAAAATCTCCG-3'.

Enzyme-linked immunosorbent assay (ELISA)

Pretreated NSCLC cells were cultured in DMEM medium without fetal bovine serum. Overnight, Supernatant of conditioned medium was collected for VEGFA-ELISA analysis according to its instructions. The absorbance was set to 450 nm, and the OD values in the sample was obtained.

Luciferase reporter assays

Pretreated NSCLC cells were seeded onto 48-well plates and transfected with the following: HIF1α promoter-luciferase reporter plasmid (PGL3-HIF1α promoter) and Renilla luciferase control vector. Transfected cells were exposed 1% O_2 for 24 h. Firefly luciferase and Renilla luciferase activities in cell lysates were determined using the Dual-Luciferase Assay System (Promega).

Tube formation assay

Pretreated NSCLC cells were cultured in DMEM medium without fetal bovine serum. The matrigel was plated in a 96-well plate. Approximately 20000 HUVECs were added to each well and incubated in NSCLC cell-conditioned medium for 24 h. Microscopic images of tube formation was assessed.

Wound healing and transwell assays

HCC827 and H460 cells were grown to 95% confluency. A linear wound was made by a 200-

μm sterile plastic pipette tip, 24 hr after treatment by mitomycin C (10 μg/ml). Cells were washed twice using PBS. Then, size of wounds were observed and measured at the indicated times. For the Matrigel invasion assays, polycarbonate membrane Transwell chambers containing a filter with a diameter of 6.5 mm diameter and 8 μm pores (Corning Inc., Corning, NY, USA). The Transwell filter was precoated or left uncoated with basement membrane Matrigel (BD Biosciences, San Jose, CA, USA). Briefly, HCC827 and H460 cells were pretreated for 24 hours. 5×10^4 cells in 300 ul of serum-free DMEM were seeded onto the upper chamber of the Transwell chamber. The lower chamber of the Transwell contained DMEM supplemented with 10% FBS, which acted as a chemoattractant for the cells. The cells were then incubated for 24 hours in a humidified incubator, at 37°C and 5% CO_2. Following this incubation, all non-invasive cells on the upper surface of the Transwell chamber were discarded. Next, the cells on the lower surface of the filter were fixed with 4% formaldehyde at room temperature for 30 minutes and then stained with 0.5% crystal violet for 20 min at room temperature. The filter was then washed three times with 1×PBS and the cells on the lower side of the filter were visualized and imaged with a inverted microscope at a ×100 magnification. This assay was done in triplicate.

Colony formation assay

500 pretreated cells were seeded into the 6-well plates. The medium was replaced every three days for approximately two weeks. Photographs of colonies were obtained using a microscope.

Mouse xenograft tumor assay

All experiments involving the mouse models were approved by the Animal Care and Use committee of Tongji Hospital. Four weeks old, male, nude mice were obtained from Beijing Huafukang Bioscience Company. 1×10^6 HCC-827 cells, stably expressing the vector, KDM4C, KDM4C+shHIF1α#1 and KDM4C+shHIF1α#2 were suspended in 200 ul of Matrigel and xenografted into nude mice subcutaneous injections into the left flank. Tumor volumes were measured every 3 days. All mice were sacrificed three weeks after xenografting.

Statistical analysis

All data were analyzed using SPSS 20.0 software. Differences were analyzed by the Student t test for two groups and by ANOVA for multiple groups. $P<0.05$ was considered significant.

Result

KDM4C is upregulated in NSCLC

To characterize the expression of KDM4C in NSCLC, we first analyzed the Oncomine database. This analysis revealed KDM4C overexpression in NSCLC tumors relative to matching paracancerous tissues. To experimentally verify this observation, we used RT-qPCR and western blotting to establish expression levels of KDM4C in our NSCLC patient tumor tissues, as well as their matched normal control tissue. These analyses revealed that KDM4C expression was significantly elevated in clinical NSCLC tissue, confirming the results from our Oncomine database analysis (**Figure 1A-D**). These findings were further supported by immunohistochemical analysis (**Figure 1E**). Statistical analysis proved that the tumor tissues had a significantly higher level of KDM4C expression ($P<0.0001$) than the matching paracancerous tissues (**Table 1**). These findings implied that the occurrence and progress of NSCLC were regulated by KDM4C.

KDM4C promoted cell proliferation, migration and invasion of NSCLC cells

Based on our observation overexpression of KDM4C in NSCLC patient tissue, we wondered whether the increased levels of KDM4C influence tumor processes like proliferation, migration and invasion in NSCLC. To address this question we stably transfected the human NSCLC cell lines HCC827 and H460, with pcDNA-3.1(+)-KDM4C plasmid and with pcDNA-3.1(+) (empty vector) as negative control. KDM4C overexpression by transfected cells was confirmed by western blot analysis (**Figure 2A**). To establish whether overexpression of KDM4C promoted cell cycle progression and cell proliferation, we stained the stably transfected cells with PI and and carried cell proliferation analysis using the CCK8 assay. KDM4C knockdown dramatically increased the G0/G1-phase ratios and reduced the S-phase

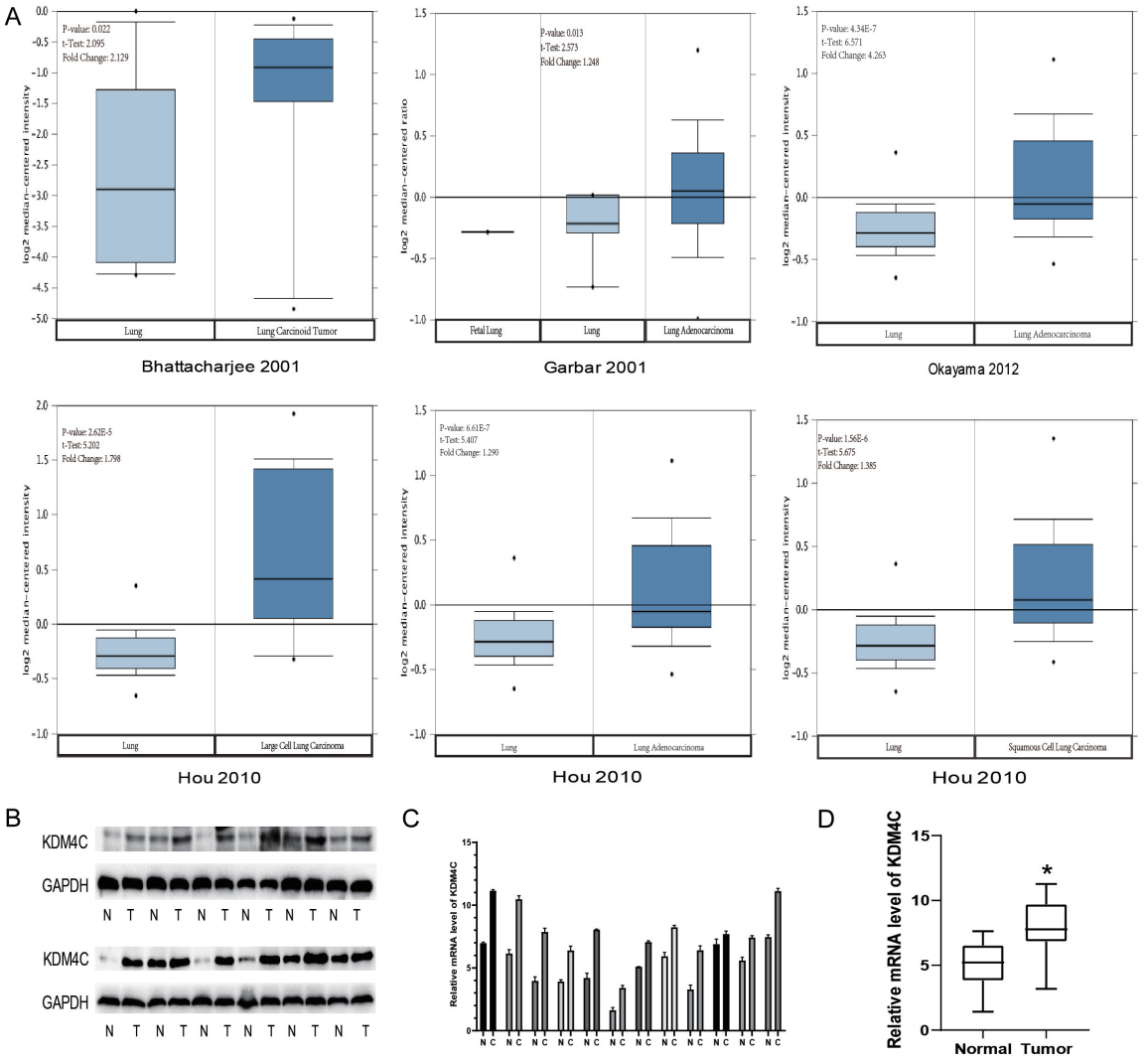

Figure 1. KDM4C expression is upregulated in NSCLC. A. KDM4C expression level in normal VS NSCLC tissues was analyzed in the Oncomine public data set. B. KDM4C expression in normal and matched paracancerous NSCLC tissues was quantified through western blot. C, D. mRNA expression in normal and matched paracancerous NSCLC tissues was detected by RT-qPCR. *; P<0.01. E. KDM4C expression in normal and NSCLC tissues was analyzed by IHC.

Table 1. The KDM4C expression level of NSCLC tissue was higher than normal tissues (P<0.0001, by Chi-square)

Variables	Cases	KDM4C		*p*-value
		high	low	
Normal	80	22	58	<0.0001
Tumor	80	38	44	

ratios. These analyses revealed that proliferation was significantly higher in KDM4C overexpressing HCC827 and H460 cells when compared to control cells (**Figure 2B**, **2C**). We next wondered whether KDM4C might promote cancer cell transformation. To address this question, we carried out a colony formation assay. This analysis revealed that relative to negative control cells, KDM4C overexpressing cells produced a significantly higher number of colonies, which also achieved significantly higher colony sizes (**Figure 2D**). These results suggested that KDM4C overexpressing cells had a more active

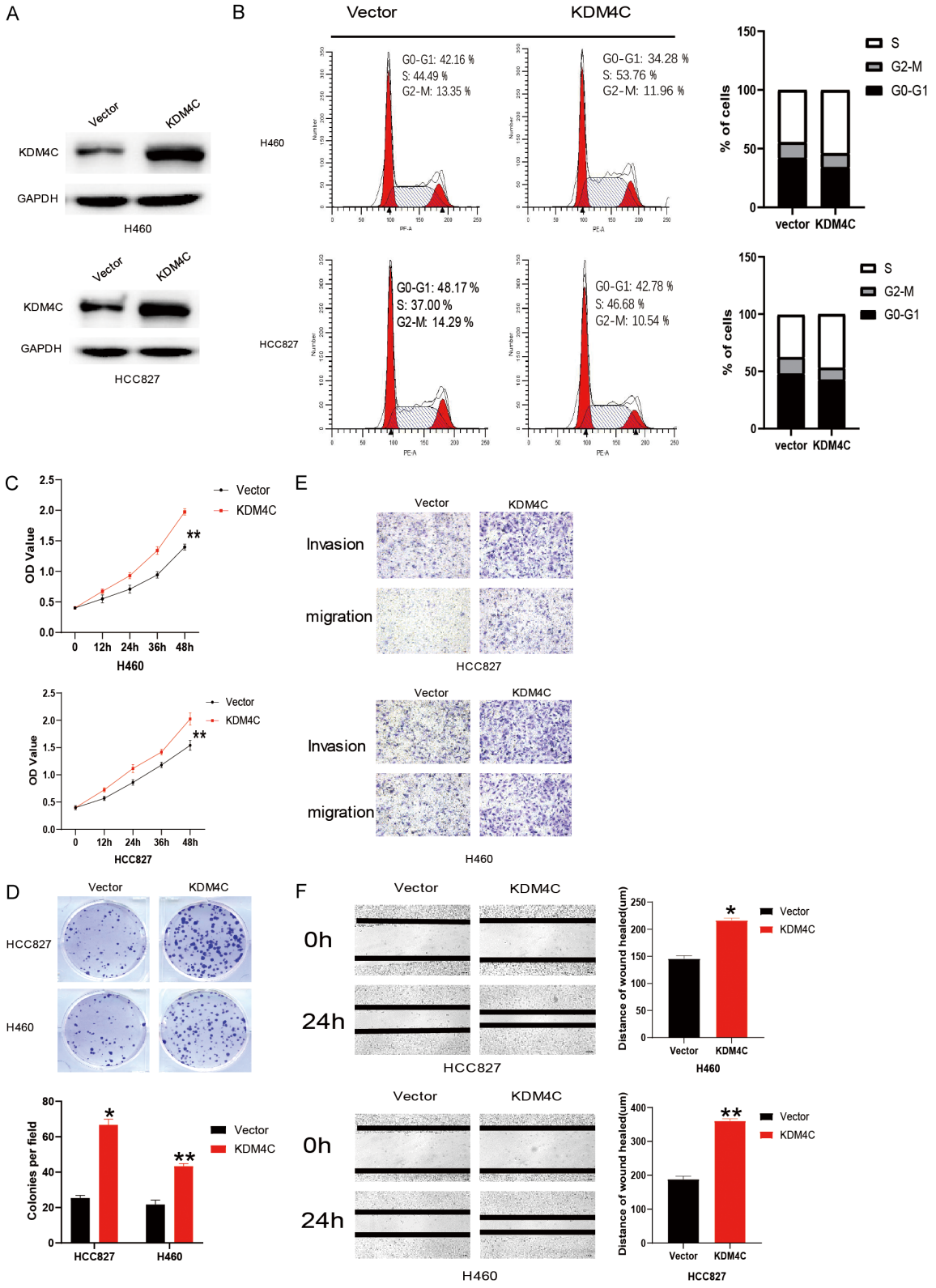

Figure 2. KDM4C promotes the cell proliferation, migration and invasion of NSCLC cells. A. H460 and HCC827cells were transfected with vector only or with KDM4C carrying vector. KDM4C expression was subsequently analyzed by western blotting. B. Cell cycle distribution was analyzed by flow cytometry in KDM4C overexpressing HCC827 and H460 cells. C. The viability and proliferation rates of HCC827 and H460 cells stably expressing the vector only or KDM4C were analyzed by the CCK8 assay. D. The colony formation assay was carried out on HCC827 and H460

cells stably expressing the empty vector or KDM4C. *; P<0.001 **; P<0.01. E, F. The migration ability of HCC827 and H460 cells stably expressing the empty vector or KDM4C was analyzed by Transwell analysis as well as through a wound healing assay. *; P<0.01 **; P<0.01.

DNA replication compared with the negative control cells.

The observation that KDM4C overexpression enhanced the ability of NSCLC cells to form colonies, leading us to hypothesize that this behavior was also likely to promote metastasis. To test this possibility, we carried out an invasion assay and compared the invasion and migration ability of KDM4C overexpressing cells relative to the negative control cells. This analysis revealed KDM4C enhanced the ability of cells to migrate and invade Matrigel (**Figure 2E**). This property of KDM4C was also confirmed by wound healing assays (**Figure 2F**). Together, these observations indicated that KDM4C promoted cell proliferation, migration and invasion by NSCLC cells.

KDM4C knockdown inhibited proliferation, migration and invasion of NSCLC cells

To further interrogate the function of KDM4C in cell proliferation, migration and invasion of NSCLC cells, we stably knocked down KDM4C in HCC827 and H460 cell lines using two different lentivirus-mediated shRNAs. Downregulation of KDM4C expression was confirmed by western blot analysis (**Figure 3A**). To establish the effect of KDM4C knockdown on cell proliferation and the cell cycle, we carried out a CCK8 assay and PI analysis respectively. This analysis revealed that loss of KDM4C suppressed the proliferation of NSCLC cells (**Figure 3B**, **3C**). Furthermore, we observed that knocking KDM4C inhibited the ability of these cells to form colonies (**Figure 3D**). To investigate the effect of silencing KDM4C on NSCLC metastasis, we carried out a Transwell assay. This analysis revealed that silencing KDM4C inhibited the ability of NSCLC cells to migration and invade. This observation was further confirmed by the wound healing assay (**Figure 3E**, **3F**). Together, these observations agreed with the KDM4C overexpression observation and indicated that KDM4C was required for proliferation, migration and invasion by NSCLC cells.

The novel role of KDM4C in the tumor angiogenesis of NSCLC cells

Tumor progression was promoted by tumor angiogenesis, which provided the nourishment that supports tumor growth. A previous study showed that KDM4C might activate the HIF-1/VEGFA signaling pathway. We therefore wondered whether the HIF-1/VEGFA signaling pathway played and important role in NSCLC. To interrogate this, we evaluated the relationship HIF-1/VEGF signaling pathway and KDM4C in NSCLC cells. To interrogate this, we used ELISA to analyze VEGFA concentration in the supernatant of cultured NSCLC cell lines. This analysis showed that increased KDM4C expression actived HIF1α/VEGFA signal pathway enhanced VEGFA secretion (**Figure 4A**, **4B**). On the contrary, reduced KDM4C expression inhibited HIF1α/VEGFA signal pathway and VEGFA secretion (**Figure 4C**, **4D**). Of note, this analysis revealed that high KDM4C expression promoted HIF1α expression but not HIF-1β and activated the HIF1α/VEGFA signaling pathway during hypoxia.

To further investigate KDM4C function in tumor angiogenesis, we performed a tube formation assay. To this end, we incubated HUVECs with conditioned media (CM) and transfected them with empty vector plasmid as negative control, KDM4C plasmid, shnc and shKDM4C virus. This analysis revealed that as expected, cells overexpressing KDM4C had a higher tube formation capacity relative to the negative control cells during hypoxia. Silencing KDM4C cells weakened tube formation ability than shnc cells in hypoxia (**Figure 4E**, **4F**). Together, these results strongly implied that KDM4C can modulate tumor angiogenesis through the HIF1α/VEGFA signaling pathway.

HIF1α transcriptional activation via demethylation of H3K9me3 and H3K36me3 by KDM4C

To further explore the mechanisms through which KDM4C modulates HIF1α/VEGFA signaling pathway, we performed a rescue experiment using KDM4C plasmid in shKDM4C knockdown cells. This experiment revealed that overexpression of KDM4C reversed the suppression of HIF1α/VEGFA signaling upon shKDM4C knockdown (**Figure 5A**).

KDM4C was one of various histone demethylases, that could demethylate H3K9me3 and H3K36me3 and affect the expression of downstream genes. We therefore wondered whether

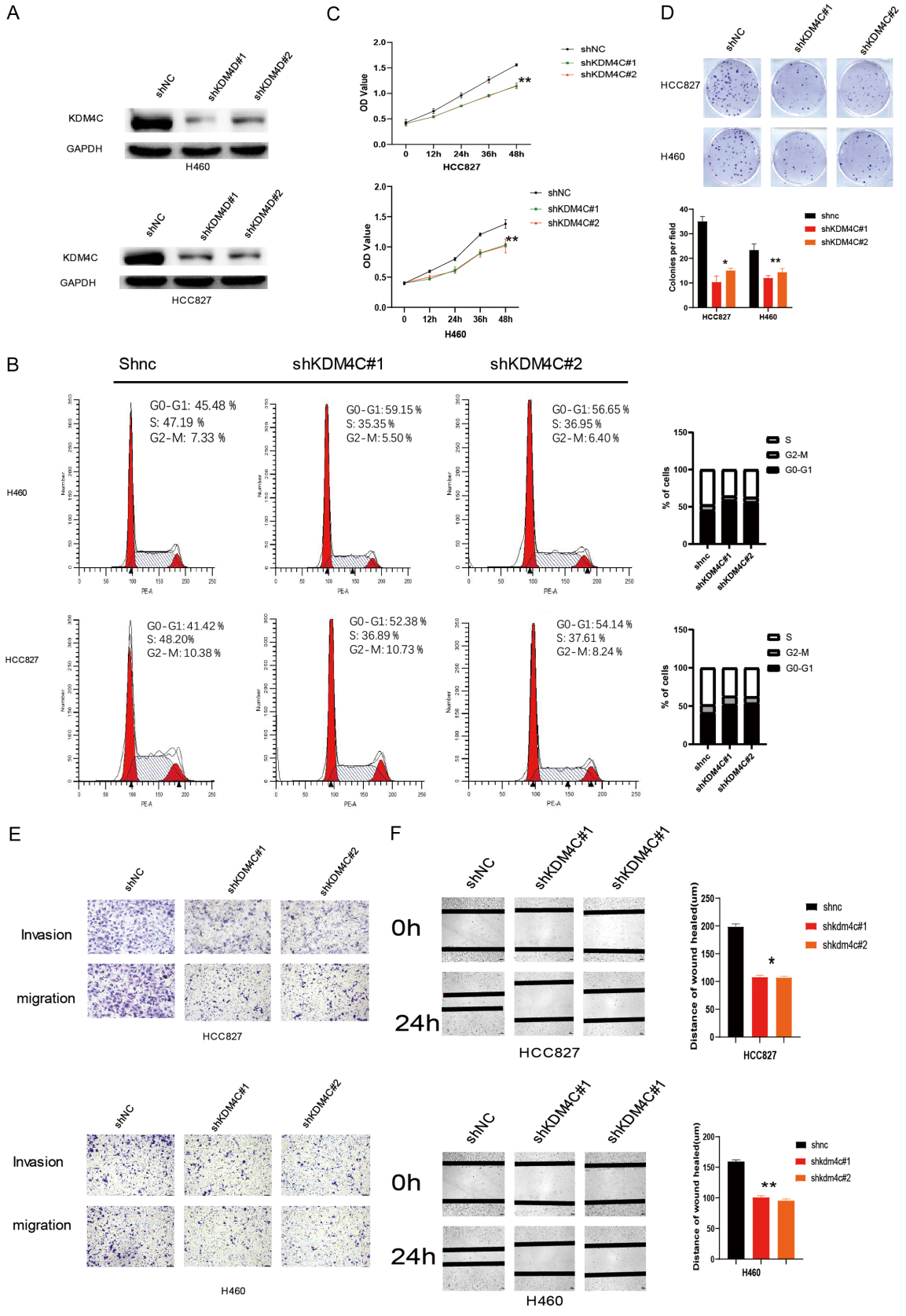

Figure 3. KDM4C knockdown inhibits cell proliferation, migration and invasion of NSCLC cells. A. H460 and HCC827 cells were transfected with shnc and shKDM4C virus and KDM4C protein levels measured by western blot analysis.

B. Cell cycle distribution was analyzed by flow cytometry in shKDM4C HCC827 and H460 cells. C. The viability of HCC827 and H460 cells stably expressing shnc and shKDM4C was analyzed by CCK8 assay. D. A colony formation assay was carried out using HCC827 and H460 cells stably expressing shnc and shKDM4C. *; P<0.01 **; P<0.01. E, F. The migration ability HCC827 and H460 cells stably expressing shnc and shKDM4C was analyzed by Transwell assay and the wound healing assay. *; P<0.01 **; P<0.01.

KDM4C affected HIF1α/VEGFA signaling pathway by demethylating H3K9me3 and H3K27me3 on the HIF1α gene promoter. To address this possibility we used western blot analysis to measure the level of H3K9me3 and H3K27me3 in KDM4C overexpressing or KDM4C knockdown cells lysate relative to negative control (empty vector) cells. This analysis revealed that KDM4C overexpressing cells had lower amounts of H3K9me3 and H3K27me3 when compared to negative control cells. Conversely, KDM4C knockdown cells revealed higher level of H3K9me3 and H3K27me3 (**Figure 5B-E**). This consistent observation of an association between the levels of HIF1α, H3K9me3, H3K27me3 and KDM4C expression led us to hypothesize that KDM4C regulated HIF1α/VEGFA signaling by demethylating H3K9me3 and H3K27me3 of the HIF1α gene promoter. To test this hypothesis we performed a chromatin immunoprecipitation (Chip) assay in order to establish whether there is an interaction between KDM4C and HIF1α gene promoter. This analysis revealed that anti-KDM4C antibody could directly immunoprecipitate the HIF1α gene promoter. We next used anti-H3K9me3 and anti-H3K27me3 antibodies for further Chip analysis. These exoeriments revealed that KDM4C overexpressing cells weakened the interaction between HIF1α gene promoter and H3K9me3 and H3K27me3 relative to the negative (empty vector) controls. Conversely, silencing KDM4C enhanced the interaction between HIF1α gene promoter and H3K9me3 and H3K27me3 relative with shnc cells (**Figure 5G**, **5H**). To further test this hypothesis, we carried out a dual-luciferase assay to detect whether KDM4C activated the HIF1α gene promoter. As expected, this assay revealed that KDM4C expressing cells had a higher ability to active HIF1α gene promoter releative to negative control cells. Conversely, shKDM4C cells revealed an inhibition of HIF1α gene promoter activation relative to shnc cells (**Figure 5I**, **5J**). Taken together, these results demonstrated that KDM4C transcriptionally modulates HIF1α expression via demethylation of H3K9me3 and H3K27me3 at promoter region in NSCLC cells.

KDM4C regulated HIF1α expression through the costimulatory factor STAT3

VEGF had been reported to be a common downstream target of STAT3 and HIF1 during hypoxia. Inhibition of STAT3 phosphorylation at Y705 suppressed HIF1α expression [21]. These observations implied that STAT3 phosphorylation at Y705 was associated with HIF1α expression. We therefore hypothesized that p-Y705-STAT3 functioned as a costimulatory factor during the regulation of HIF1α expression by KDM4C. To test this hypothesis, we performed a co-IP analysis to establish whether there was interaction between KDM4C and STAT3 (**Figure 6A**, **6B**). A Chip analysis showed that the HIF1α gene promoter was directly immunoprecipitated by the anti-STAT3 antibody (**Figure 6C**). Anti-H3K9me3 and anti-H3K27me3 antibodies were used for further Chip analysis in STAT3 overexpressing cells. This analysis revealed that STAT3 overexpression weakened the interaction between the HIF1α gene promoter and H3K9me3 and H3K27me3 relative to the negative controls (**Figure 6E**). Conversely, shSTAT3 cells or S3I-201, an inhibitor of STAT3 Y705 phosphorylation, enhanced the interaction between HIF1α gene promoter and H3K9me3 and H3K27me3 relative to shnc cells or DMSO (**Figures 6D** and S1A-D). To further interrogate the function of STAT3 as a costimulatory factor, we performed a dual-luciferase assay so as to determine if STAT3 activates HIF1α gene promoter. These experiments revealed that STAT3 overexpressing cells enhance HIF1α gene promoter activation when compared to negative control cells (**Figure 6F**). In contrast, shSTAT3 cells or pharmacologically inhibiting STAT3 Y705 phosphorylation inhibited HIF1α gene promoter activation relative to shnc cells or DMSO treated cells (**Figures 6G** and S1E). Together, these experiments indicated that STAT3 functions as a costimulatory factor in the regulation HIF1α expression by KDM4C. Knockdown of STAT3 or pharmacologic inhibition of STAT3 Y705 phosphorylation impaired the modulation HIF1α/VEGFA signaling pathway by KDM4C by increasing the interation between H3K9me3, H3K36me3 and HIF1α gene promoter.

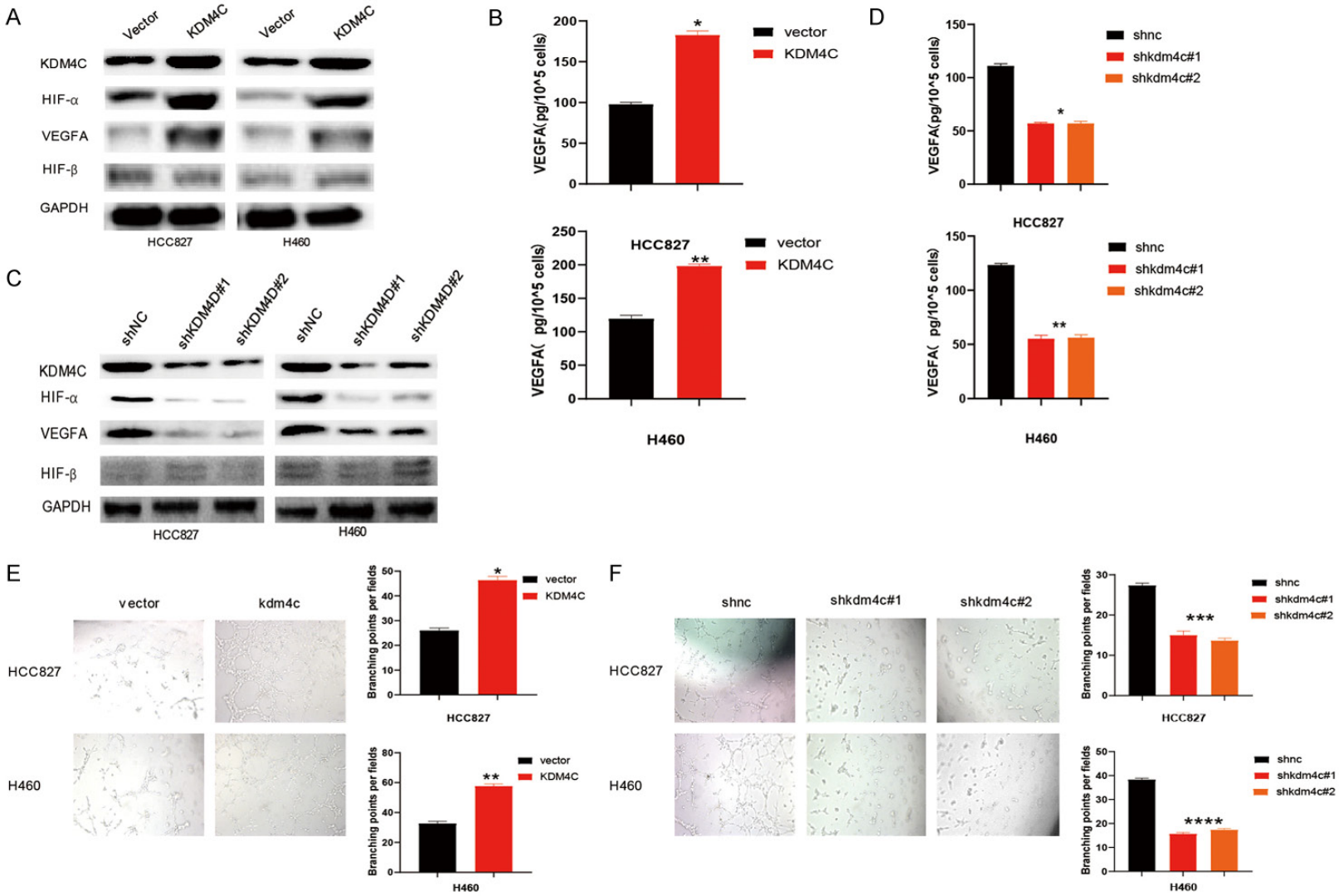

Figure 4. KDM4C promotes tumor angiogenesis of NSCLC cells by activating the HIF1α/VEGFA signal pathway. A. The levels of HIF1α, HIF1β and VEGFA proteins were analyzed by western blotting in HCC827 and H460 cells stably expressing the empty vector or KDM4C durinf hypoxia. B. HCC827 and H460 cells stably expressing the empty vector or KDM4C were cultured in serum free DMEM in hypoxic conditions overnight. On the next day, the supernatants of conditioned media were collected for VEGFA secretion analysis through ELISA. *; P<0.01 **; P<0.01. C, D. Western blot and ELISA analysis was used to analyze HIF1α, HIF1β and VEGFA protein levels in HCC827 and H460 cells stably expressing shnc or shKDM4C in hypoxic conditions. *; P<0.01 **; P<0.01. E, F. The tube formation ability of HUVECs stably expressing the empty vector or KDM4C, shnc or shKDM4C in hypoxix conditions was analyzed through a tube formation assay. *; P<0.01 **; P<0.01 ***; P<0.01 ****; P<0.01.

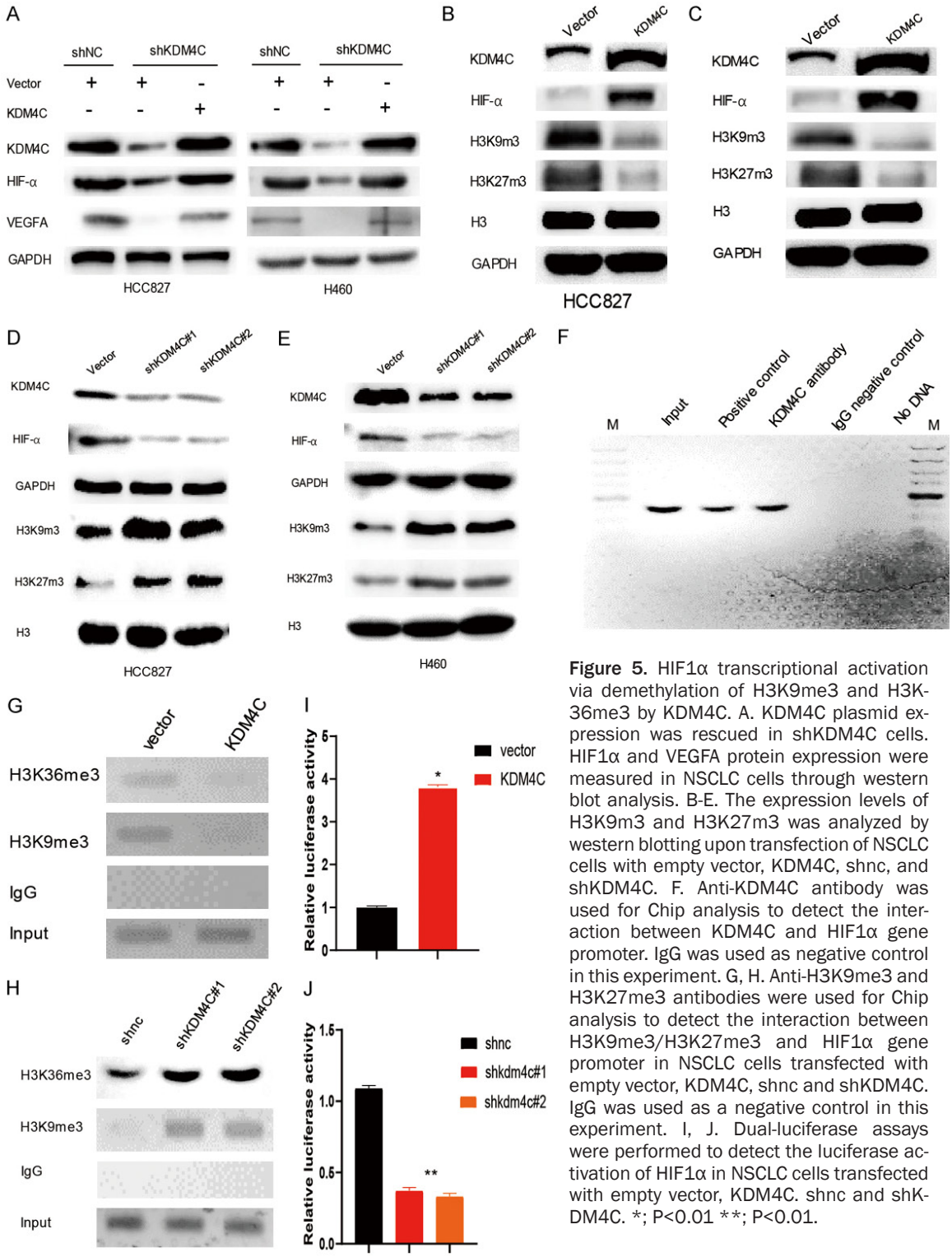

Figure 5. HIF1α transcriptional activation via demethylation of H3K9me3 and H3K-36me3 by KDM4C. A. KDM4C plasmid expression was rescued in shKDM4C cells. HIF1α and VEGFA protein expression were measured in NSCLC cells through western blot analysis. B-E. The expression levels of H3K9m3 and H3K27m3 was analyzed by western blotting upon transfection of NSCLC cells with empty vector, KDM4C, shnc, and shKDM4C. F. Anti-KDM4C antibody was used for Chip analysis to detect the interaction between KDM4C and HIF1α gene promoter. IgG was used as negative control in this experiment. G, H. Anti-H3K9me3 and H3K27me3 antibodies were used for Chip analysis to detect the interaction between H3K9me3/H3K27me3 and HIF1α gene promoter in NSCLC cells transfected with empty vector, KDM4C, shnc and shKDM4C. IgG was used as a negative control in this experiment. I, J. Dual-luciferase assays were performed to detect the luciferase activation of HIF1α in NSCLC cells transfected with empty vector, KDM4C. shnc and shKDM4C. *; P<0.01 **; P<0.01.

In vivo KDM4C regulation of angiogenesis was dependent on HIF1α

To further investigate if the role of KDM4C in tumor angiogenesis was dependent on HIF1α, we constructed HCC827 cell lines that stably expressed vector+shnc, KDM4C+shnc, KDM4C+shHIF1α#1 and KDM4C+shHIF1α#2. These four cell lines were subcutaneously injected into the backs of 4 weeks old Balb/c nude

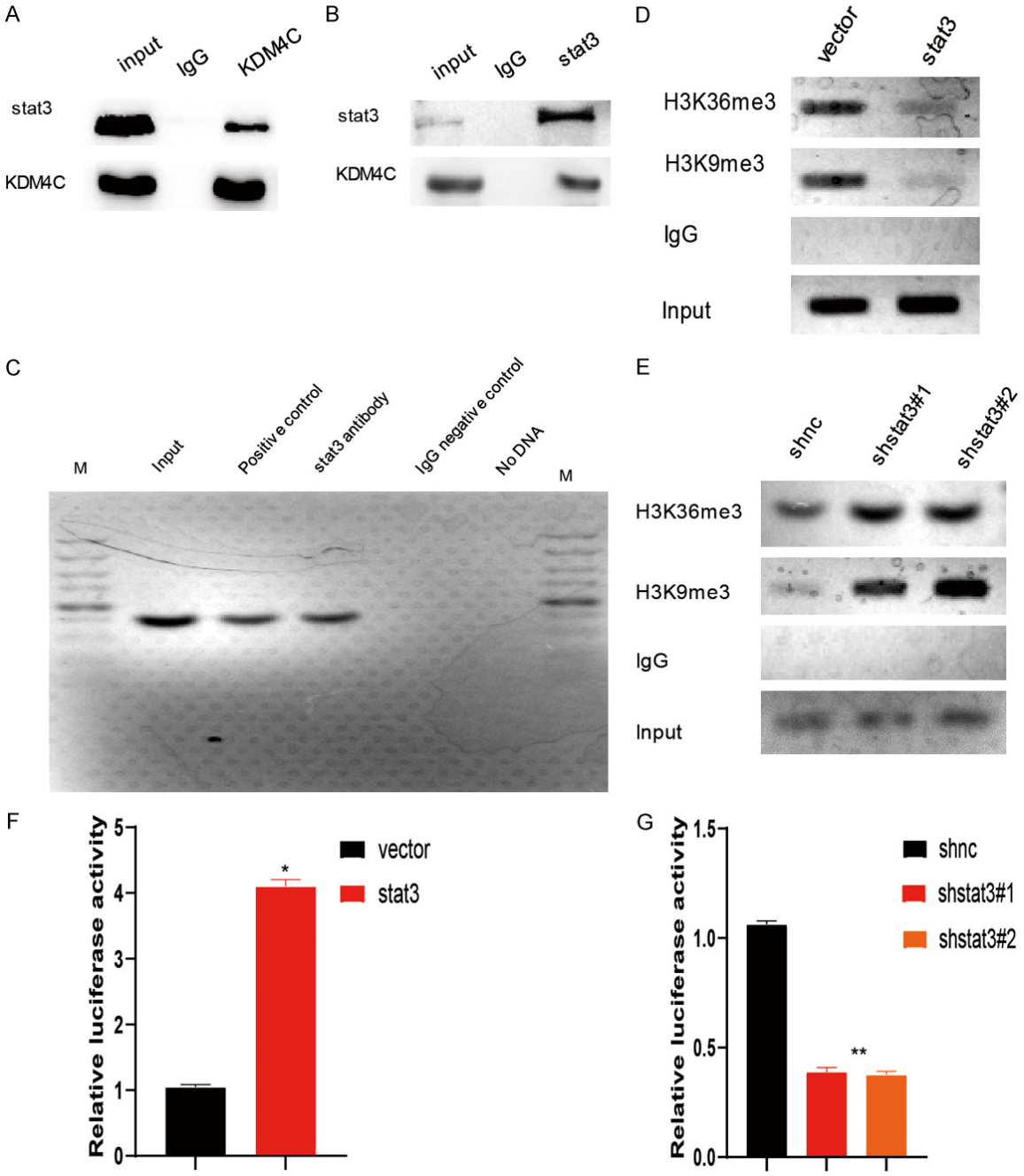

Figure 6. KDM4C regulates HIF1α expression through the costimulatory factor STAT3. A, B. Whole-cell extracts of HEK293 cells were collected for IP analysis using the indicated antibodies, followed by IB analysis. C. anti-STAT3 antibody was used for Chip analysis to detect interaction between STAT3 and HIF1α gene promoter in HCC827 cells. IgG was used as a negative control in this experiment. D, E. Anti-H3K9me3 and H3K27me3 antibody were used for CHIP analysis to detect the interaction between H3K9me3/H3K36me3 and HIF1α gene promoter in NSCLC cells carryin the empty vector, STAT3, shnc and shSTAT3. IgG was used as negative control. F, G. Dual-luciferase assay-swere applied to detect the luciferase activation of HIF1α in NSCLC cells transfected with empty vector, STAT3, shnc and shSTAT3. *; P<0.01 **; P<0.01.

mice. This analysis revealed that KDM4C cells grew significantly faster than negatice (empty vector) control cells. However, KDM4C+shHIF-1α cells suppressed the promotion tumor growth by KDM4C. Moreover, the size and weights of the tumors were significantly higher in KDM4C overexpressing tumors than in the negative control tumors. This effect was

impaired by knockdown of HIF1α gene expression (**Figure 7A-C**). To examine state of angiogenesis status in the xenografted tumors, we performed IHC to determine the expression levels of CD31 in the various xenograft groups. From this analysis, the expression levels CD31 were clearly elevated in the KDM4C overexpressing group relative to the negative control group in which it was impaired by silencing HIF1α (**Figure 7D**, **7E**). This observation indicated that the ability of KDM4C to promote tumor angiogenesis was suppressed as a consequence of HIF1α gene silencing in NSCLC. Consistently, western blot analysis revealed that VEGFA expression level was significantly increased in the KDM4C group relative to the negative control group. Silencing HIF1α reversed the VEGFA expression levels that were elevated by KDM4C overexpression (**Figure 7F**). Taken together, our study demonstrated that KDM4C promotion of tumor angiogenesis in vivo was HIF1α dependent.

Discussion

Histone methylation, a process regulated by specific histone methyltransferases and histone demethylases, controlled gene expression processes, therefore modulating a wide range of cellular processes including cell proliferation, differentiation and apoptosis [17]. Misregulation of this processes was linked with tumorigenesis. Here, we reported the that the expression level of KDM4C, a member of the KDM superfamily of histone demethylases, was markedly elevated in NSCLC tissues than in the matched normal tissue both in GEO datasets and in clinical NSCLC tissues (**Figure 1**). Our study also revealed that the expression levels of KDM4C were positively correlated with NSCLC cell proliferation rate as well as their migration, and invasion ability (**Figures 2** and **3**). Together, these results indicated that KDM4C expression levels influenced the rate of tumor progression in NSCLC.

The HIF/VEGFA signaling pathway had been previously reported to be activated in many tumors, included NSCLC [22]. Anti-angiogenic therapy, a novel therapeutic strategy had been applied in the treatment of various types of aggressive malignant tumors (insert reference). Therapeutic strategies against VEGFs significantly decreased tumor proliferation, invasion, and migration. Previous studies had shown that during hypoxia HIF-1α stabilized and dimerized with HIF-1β as a consequence of low O_2 levels. This in turn, activates HIF target gene expression through interaction with the co-activator CBP/p300 [23]. In a previous study in breast cancer cells, KDM4C was demonstrated to modulate HIFs/VEGF signaling pathway by upregulating HIF1β but not HIF1α [20]. On the contrary, in this study, we found that during hypoxia, KDM4C modulated the HIF/VEGFA signaling pathway by increasing HIF1α expression but not HIF1β expression in NSCLC cells. This discrepancy might be a reflection of the different biology exhibited by the different cell lines used in this study. In addition, the use of different experimental methods might contribute to this contrasting observation. In this study, we found that upregulated KDM4C expression activated the HIF1α/VEGFA signaling pathway, and significantly enhanced HUVEC tube formation (**Figure 4**).

KDM4C had been shown to demethylate H3K9me3 and H3K36me3 on the promoter regions of target genes, thereby functioning as a transcriptional regulator [14]. In this study, we found that KDM4C affects H3K9, H3K27 methylation and also bind to the HIF1α promoter. In addition, Chip assays showed that KDM4C expression levels significantly affected the interaction between H3K9m3, H3K36m3 and HIF1α promoter (**Figure 5**). STAT3, a transcription factor, has been shown to modulate the expression of target genes and a previous study reported that PKR inhibits HIF-1α expression by impairing STAT3 phosphorylation at Y705 [9]. In this study, we find that KDM4C interacts with STAT3. Interestingly, Chip analyses showed that STAT3 interacts with the HIF1α promoter and that the level of STAT3 expression or the level of STAT3 phosphorylation at Y705 strongly affected the interaction between H3K9m3, H3K36m3 and HIF1α, observations that were consistent with those made for KDM4C (**Figures 6** and S1). Moreover, compared to NSCLCs cells carrying an empty vector, cells overexpressing KDM4C resulted in bigger tumors when xenografted into Balb/c nude mice and this corresponded with increased VEGFA expression and tumor angiogenesis. Silencing HIF1α impaired KDM4C promotion of tumor angiogenesis (**Figure 7**).

In conclusion, this study revealed a novel insight, that KDM4C regulated the HIF1α/VEGFA signaling pathway in association with

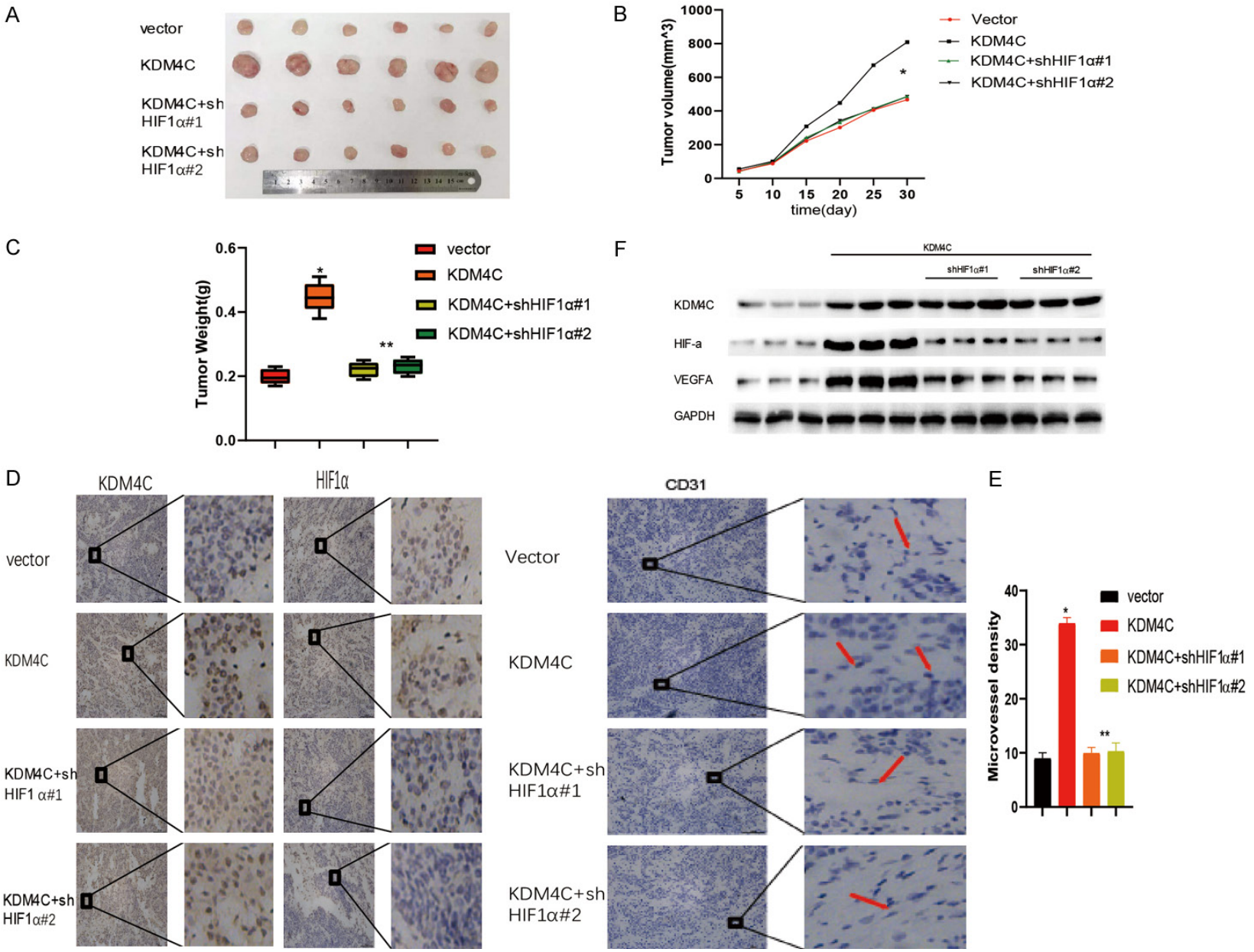
A
vector
KDM4C
KDM4C+sh HIF1α#1
KDM4C+sh HIF1α#2
B
Tumor volume(mm^3)
time(day)
Vector
KDM4C
KDM4C+shHIF1α#1
KDM4C+shHIF1α#2
C
Tumor Weight(g)
vector
KDM4C
KDM4C+shHIF1α#1
KDM4C+shHIF1α#2
F
KDM4C
shHIF1α#1
shHIF1α#2
KDM4C
HIF-a
VEGFA
GAPDH
D
KDM4C
HIF1α
CD31
vector
KDM4C
KDM4C+sh HIF1 α#1
KDM4C+sh HIF1α#2
Vector
KDM4C
KDM4C+sh HIF1α#1
KDM4C+sh HIF1α#2
E
Microvessel density
vector
KDM4C
KDM4C+shHIF1α#1
KDM4C+shHIF1α#2

Figure 7. In vivo KDM4C regulation of angiogenesis is dependent on HIF1α. A. HCC827 cells stably expressing vector, KMD4C, shHIF1α#1 or shHIF1α#2 were subcutaneously injected into the backs of 4 weeks old Balb/c nude mice. The mice were sacrificed after 28 days. Representative tumor images at the end of the experiment are shown. B. Tumor weights and sizes were examined in the four groups. *; P<0.01. C. Tumor volume growth curves from day 1-28 are shown. *; P<0.01 **; P<0.01. D, E. Representative IHC staining of KDM4C and CD31 in the two groups are shown. The right histogram shows tumor microvessel density in the four groups. *; P<0.01 **; P<0.01. F. The Indicated protein expression levels in xenograft tumors were measured by western blot analysis.

the costimulatory factor STAT3, thereby promoting tumor angiogenesis. These findings advanced our understanding of the molecular basis of NSCLC and might elucidate novel therapeutic avenues against this disease.

Acknowledgements

This work was financially supported by the grants from National Natural Sciences Foundation of China (NO. 81700174; NO. 81802160).

Disclosure of conflict of interest

None.

Address correspondence to: Dr. Jin Yin, Department of Hematopathology, Tongji Hospital, Tongji Medical Collage of Huazhong University of Science and Technology, Wuhan, Hubei Province, China. Tel: +86-027-6363-9716; E-mail: evita3482@qq.com

References

[1] Murray CJ and Lopez AD. Mortality by cause for eight regions of the world: global burden of disease study. Lancet 1997; 349: 1269-1276.

[2] Foreman KJ, Marquez N, Dolgert A, Fukutaki K, Fullman N, McGaughey M, Pletcher MA, Smith AE, Tang K, Yuan CW, Brown JC, Friedman J, He J, Heuton KR, Holmberg M, Patel DJ, Reidy P, Carter A, Cercy K, Chapin A, Douwes-Schultz D, Frank T, Goettsch F, Liu PY, Nandakumar V, Reitsma MB, Reuter V, Sadat N, Sorensen RJD, Srinivasan V, Updike RL, York H, Lopez AD, Lozano R, Lim SS, Mokdad AH, Vollset SE and Murray CJL. Forecasting life expectancy, years of life lost, and all-cause and cause-specific mortality for 250 causes of death: reference and alternative scenarios for 2016-40 for 195 countries and territories. Lancet 2018; 392: 2052-2090.

[3] Ettinger DS, Aisner DL, Wood DE, Akerley W, Bauman J, Chang JY, Chirieac LR, D'Amico TA, Dilling TJ, Dobelbower M, Govindan R, Gubens MA, Hennon M, Horn L, Lackner RP, Lanuti M, Leal TA, Lilenbaum R, Lin J, Loo BW, Martins R, Otterson GA, Patel SP, Reckamp K, Riely GJ, Schild SE, Shapiro TA, Stevenson J, Swanson SJ, Tauer K, Yang SC, Gregory K and Hughes M. NCCN guidelines insights: non-small cell lung cancer, version 5.2018. J Natl Compr Canc Netw 2018; 16: 807-821.

[4] Goel HL and Mercurio AM. VEGF targets the tumour cell. Nat Rev Cancer 2013; 13: 871-882.

[5] Giaccia A, Siim BG and Johnson RS. HIF-1 as a target for drug development. Nat Rev Drug Discov 2003; 2: 803-811.

[6] Semenza GL. Defining the role of hypoxia-inducible factor 1 in cancer biology and therapeutics. Oncogene 2010; 29: 625-634.

[7] Semenza GL. Hypoxia-inducible factors in physiology and medicine. Cell 2012; 148: 399-408.

[8] Bromberg J and Darnell JE Jr. The role of STATs in transcriptional control and their impact on cellular function. Oncogene 2000; 19: 2468-2473.

[9] Yu H and Jove R. The STATs of cancer--new molecular targets come of age. Nat Rev Cancer 2004; 4: 97-105.

[10] Pawlus MR, Wang L and Hu CJ. STAT3 and HIF1alpha cooperatively activate HIF1 target genes in MDA-MB-231 and RCC4 cells. Oncogene 2014; 33: 1670-1679.

[11] Wang H, Byfield G, Jiang Y, Smith GW, McCloskey M and Hartnett ME. VEGF-mediated STAT3 activation inhibits retinal vascularization by down-regulating local erythropoietin expression. Am J Pathol 2012; 180: 1243-1253.

[12] Liu JF, Deng WW, Chen L, Li YC, Wu L, Ma SR, Zhang WF, Bu LL and Sun ZJ. Inhibition of JAK2/STAT3 reduces tumor-induced angiogenesis and myeloid-derived suppressor cells in head and neck cancer. Mol Carcinog 2018; 57: 429-439.

[13] Pollard PJ, Loenarz C, Mole DR, McDonough MA, Gleadle JM, Schofield CJ and Ratcliffe PJ. Regulation of Jumonji-domain-containing histone demethylases by hypoxia-inducible factor (HIF)-1alpha. Biochem J 2008; 416: 387-394.

[14] Agger K, Nishimura K, Miyagi S, Messling JE, Rasmussen KD and Helin K. The KDM4/JMJD2 histone demethylases are required for hematopoietic stem cell maintenance. Blood 2019; 134: 1154-1158.

[15] Gregory BL and Cheung VG. Natural variation in the histone demethylase, KDM4C, influenc-

es expression levels of specific genes including those that affect cell growth. Genome Res 2014; 24: 52-63.
[16] Whetstine JR, Nottke A, Lan F, Huarte M, Smolikov S, Chen Z, Spooner E, Li E, Zhang G, Colaiacovo M and Shi Y. Reversal of histone lysine trimethylation by the JMJD2 family of histone demethylases. Cell 2006; 125: 467-481.
[17] Berry WL and Janknecht R. KDM4/JMJD2 histone demethylases: epigenetic regulators in cancer cells. Cancer Res 2013; 73: 2936-2942.
[18] Liu G, Bollig-Fischer A, Kreike B, van de Vijver MJ, Abrams J, Ethier SP and Yang ZQ. Genomic amplification and oncogenic properties of the GASC1 histone demethylase gene in breast cancer. Oncogene 2009; 28: 4491-4500.
[19] Wissmann M, Yin N, Muller JM, Greschik H, Fodor BD, Jenuwein T, Vogler C, Schneider R, Gunther T, Buettner R, Metzger E and Schule R. Cooperative demethylation by JMJD2C and LSD1 promotes androgen receptor-dependent gene expression. Nat Cell Biol 2007; 9: 347-353.
[20] Luo W, Chang R, Zhong J, Pandey A and Semenza GL. Histone demethylase JMJD2C is a coactivator for hypoxia-inducible factor 1 that is required for breast cancer progression. Proc Natl Acad Sci U S A 2012; 109: E3367-3376.
[21] Papadakis AI, Paraskeva E, Peidis P, Muaddi H, Li S, Raptis L, Pantopoulos K, Simos G and Koromilas AE. eIF2{alpha} Kinase PKR modulates the hypoxic response by Stat3-dependent transcriptional suppression of HIF-1{alpha}. Cancer Res 2010; 70: 7820-7829.
[22] Mimura I, Nangaku M, Kanki Y, Tsutsumi S, Inoue T, Kohro T, Yamamoto S, Fujita T, Shimamura T, Suehiro J, Taguchi A, Kobayashi M, Tanimura K, Inagaki T, Tanaka T, Hamakubo T, Sakai J, Aburatani H, Kodama T and Wada Y. Dynamic change of chromatin conformation in response to hypoxia enhances the expression of GLUT3 (SLC2A3) by cooperative interaction of hypoxia-inducible factor 1 and KDM3A. Mol Cell Biol 2012; 32: 3018-3032.
[23] Lu X and Kang Y. Hypoxia and hypoxia-inducible factors: master regulators of metastasis. Clin Cancer Res 2010; 16: 5928-5935.

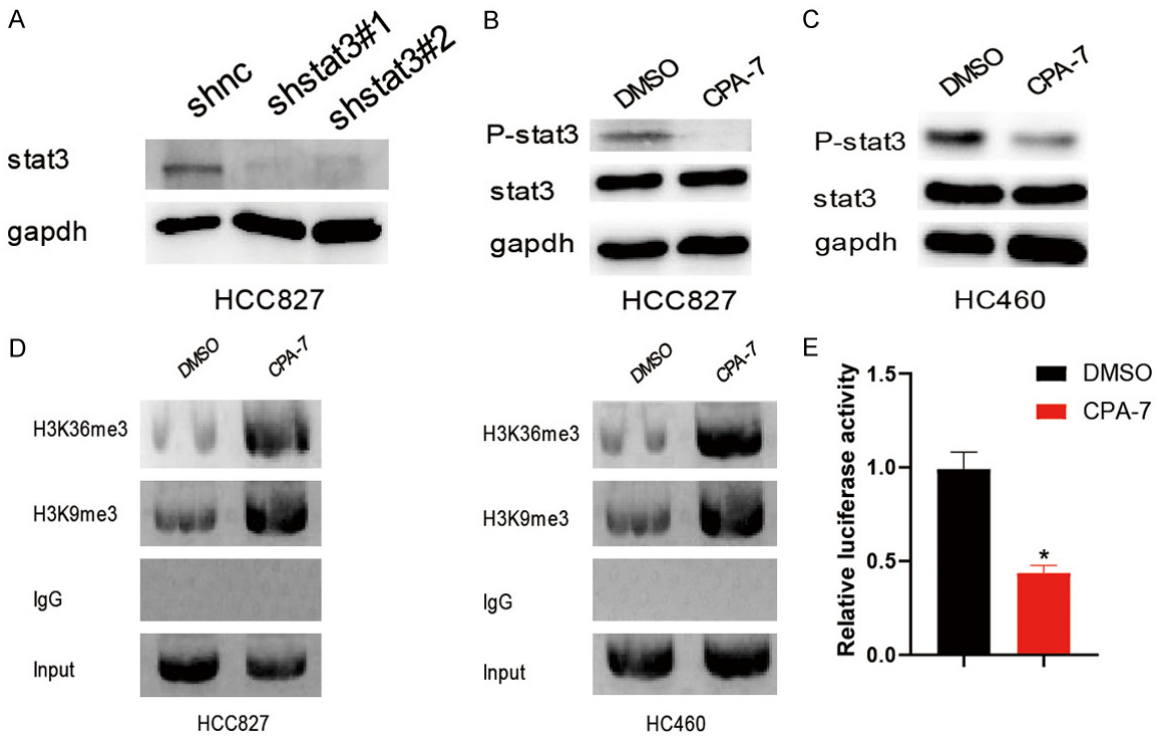

Figure S1. A. The indicated proteins were detected in HCC827 cells that stably expressed shnc, shSTAT3#1 and shSTAT3#2. B, C. HCC827 and H460 cells were treated with CPA-7 for 2 h, and STAT3 Y705 phosphorylation level detected by western blot analysis. D. Chip analysis was used to detect the interaction between STAT3 and HIF1α gene promoter in HCC827 and HC460 cells treated with CPA-7. IgG was used as negative control in this experiment. E. Dual-luciferase assays were done to detect the luciferase activation of HIF1α in HCC827 cells treated with CPA-7 for 2 h. *; P<0.01.